1-2009

Thin Films Formed by Selenization of $CuIn_xB_{1-x}$ Precursors in Se Vapor

C. A. Kamler
University of Nebraska-Lincoln

Rodney J. Soukup
University of Nebraska-Lincoln, rsoukup1@unl.edu

Natale J. Ianno
University of Nebraska-Lincoln, nianno1@unl.edu

J. L. Huguenin-Love
University of Nebraska-Lincoln

J. Olejníček
University of Nebraska–Kearney, 905 West 25th Street Kearney, NE

See next page for additional authors

Published in *Solar Energy Materials and Solar Cells* 93:1 (January 2009), pp. 45–50; doi: 10.1016/j.solmat.2008.02.027 Selected Papers from the Photovoltaics, Solar Energy Materials & Thin Films Symposium, Cancun, Mexico, August 19–23, 2007, XVI International Materials Research Congress. http://www.elsevier.com/locate/solmat

Submitted September 6, 2007; revised February 25, 2008; accepted February 26, 2008; published online April 17, 2008.

Thin films formed by selenization of $CuIn_xB_{1-x}$ precursors in Se vapor

C. A. Kamler,[a] R. J. Soukup,[a] N. J. Ianno,[a] J. L. Huguenin-Love,[a] J. Olejníček,[b] S. A. Darveau,[b] and C. L. Exstrom [b]

[a] Department of Electrical Engineering, University of Nebraska–Lincoln, 209N WSEC Lincoln, NE 68588-0511, USA
[b] Department of Chemistry, University of Nebraska–Kearney, 905 West 25th Street Kearney, NE 68849-1150, USA
Corresponding author – R. J. Soukup, tel 402 472-1980, fax 402 472-4732, email rsoukup@unl.edu

Abstract
Previous attempts in producing light absorbing materials with bandgaps near the 1.37 eV efficiency optimum have included the partial substitution of gallium or aluminum for indium in the CIS system. The most efficient of these solar cells to date have had absorber layers with bandgaps < 1.2 eV. It is logical that an even smaller substitutional atom, boron, should lead to a wider bandgap with a smaller degree of atomic substitution. In this study, copper–indium–boron precursor films are sputtered onto molybdenum coated glass substrates and post-selenized. In the selenized films, although X-ray diffraction (XRD) measurements confirm that a CIS phase is present, Auger electron spectroscopy (AES) results indicate that boron is no longer homogeneously dispersed throughout the film as it was in the case of the unselenized precursor.

Keywords: chalcopyrites, CIBS, sputtering, post-selenization

1. Introduction

A recent paper by Contreras et al. [1] has set the optimum absorber bandgap for terrestrial solar cells at 1.37 eV. In this paper they announce the highest efficiency for a chalcopyrite solar cell as 19.5%. This high efficiency is achieved with 30% Ga substitution for In within the CIGS system, yielding a bandgap of 1.14 eV. In order to attain the ideal bandgap, a substitution level of 67% Ga for In would be needed. At that level, the efficiency for CIGS solar cells is reduced to approximately 14% [1].

There are evidently several reasons for the decrease in efficiency when the Ga content becomes high enough to reach the ideal bandgap. In the above-mentioned paper the authors show that the dark current and diode ideality factor, J_0 and A, respectively, in Equation (1) below for current density, J, as a function of developed voltage, V, both increase substantially for $E_g > 1.2$ eV:

$$J = J_0 e^{q((V-RJ)/AkT)} + GV - J_L. \quad (1)$$

The other terms in this equation are the standard q, electron charge; k, Boltzmann's constant; R, series resistance; G, shunt conductance; and J_L, the light generated current density.

The authors explain the rise in A as a function of Ga content for all bandgaps as probably due to an increase in space charge region recombination. This increase in A is most likely due to changes in interface states between the CIGS and CdS or other window material, with more interface states for more Ga. The explanation for the increase in J_0 is probably associated with large changes in the electrical transport properties of the absorber (CIGS) layer. This is logically due to reductions in diffusion length due to alterations in the lattice crystal structure when Ga substitution exceeds 30%. In order to achieve a 1.37 eV bandgap, a substitution of 67% Ga would be calculated from Equation (2) below [2]:

$$E_g(x) = (1 - x)E_g(A) + xE_g(B) - bx(1 - x). \quad (2)$$

In this equation A refers to In and B refers to Ga, Al, or B. (The bowing coefficient b can be shown to have little effect on the equation.) As a consequence of the high density of Ga needed to achieve the desired bandgap and the fact that the efficiency decreases when the Ga concentration exceeds 30%, attempts have been made to increase the bandgap using aluminum as a substitution for In. Using Equation (2) above, only 25% Al would be needed to reach a bandgap of 1.37 eV.

To date, an efficiency of 16.9% has been achieved in $CuIn_xAl_{1-x}Se_2$ [3] and this is with a bandgap of about 1.15 eV with Al substituting for 13% of the In. An increase in Al content always degrades the device efficiency when compared to a CIGS cell with equal bandgap. The cause is explained to be due to significantly greater disorder in the absorber layer when the Al content is increased [4]. More recent work on this combination of materials [5] is more closely related to our efforts here. The Cu, In, and Al are deposited sequentially and selenized in an Se vapor. The resultant films do not have complete incorporation of aluminum into the $CuInSe_2$ structure, but the Al accumulates at the back of the film.

An analysis of Equation (2) using boron and an estimate of the bandgap of $CuBSe_2$ [6] yields a substitution level for B for In of only 18.6% to yield a bandgap of 1.37 eV. Unfortunately, at this time boron has not been fully introduced into the CIS structure. An analysis of the film properties and a discussion of the methods used to produce these films are in the following section.

2. Deposition techniques

All films fabricated in this study were deposited via magnetron sputtering of individual Cu, In, and *B* targets or by sputtering targets consisting of some mixture of those elements. The films were then post-selenized in a manner similar to that reported in the literature for CIGS [7, 8]. Several methods were used to deposit CuInB films onto Mo coated soda-lime glass substrates:

1. Cu and $Cu_{0.45}In_{0.55}$ were DC sputtered and boron was RF sputtered. All targets were sputtered simultaneously (sample no. 070425CIB1).
2. $Cu_{0.45}In_{0.55}$ was DC sputtered and boron was RF sputtered. Both targets were sputtered simultaneously (sample no. 070718CIB1).
3. A boron layer was RF sputtered first and a $Cu_{0.45}In_{0.55}$ layer was DC sputtered onto the boron (sample no. 070427CIB1).
4. A $Cu_{0.45}In_{0.55}$ layer was DC sputtered first and boron was RF sputtered onto the $Cu_{0.45}In_{0.55}$ (sample no. 070810CIB1).
5. Cu_3B_2 and $Cu_{0.45}In_{0.55}$ targets were DC sputtered simultaneously (sample no. 070806CIB1).

Specific deposition parameters are detailed in the table. In these depositions the substrates were all at the temperature of the sputtering system with no additional heating. The layered samples are indicated by Cycles #1 and #2. The background pressure was always less than 1.3×10^{-4} Pa and all deposition took place at approximately 0.27 Pa. In each case, the substrate to target distance was 5 cm. Auger electron spectroscopy (AES) and/or XRD were used to analyze these films. The results are discussed below (Table 1).

3. Results

3.1. Deposition and study of precursors and selenized films

The first CIB precursor film was made by co-sputtering Cu, $Cu_{0.45}In_{0.55}$, and B. The Auger depth profile in Figure 1 shows the atomic concentration for precursor sample 070425CIB1. The film was then subjected to an ex situ selenization procedure similar to that found in the literature for CIS [7] and CIGS [8]:

(1) The film, residing in a graphite boat with selenium reservoirs in a rough vacuum environment (~1 Pa), was heated to a temperature of 250 °C at a rate of 25 °C/min.

(2) The temperature was held at 250 °C for 20 min.

(3) The temperature was increased to 400 °C at a rate of 30 °C/min.

(4) The temperature was held at 400 °C for 30 min.

The purpose of steps 1 and 2 are to evaporate the Se to form a thin layer on the film surface. Steps 3 and 4 drive the Se into the film and allow the bonding reactions to take place. Several

Table 1. Precursor deposition parameters

Sample	Sputter time (min)		Cu(0.45) In(0.55)	Cu(0.4) B(0.6)	Cu	B	Cu (AES)	In (AES)	B (AES)
	Cycle #1	Cycle #2	DC current (mA)	DC current (mA)	DC current (mA)	RF power (W)	(%)	(%)	(%)
070810CIB1	32 (CuIn)	225 (B)	208			150	NA	NA	NA
070806CIB1	58	NA	100	163.5			45.00	27.50	27.50
070718CIB1	98	NA	60			150	22.50	22.50	55.00
070425CIB1	186	NA	45		35	150	58.00	14.00	28.00
070228CI1	40	NA	100				45.00	55.00	0
070427CIB1	223 (B)	16 (CuIn)	100			150	NA	NA	NA

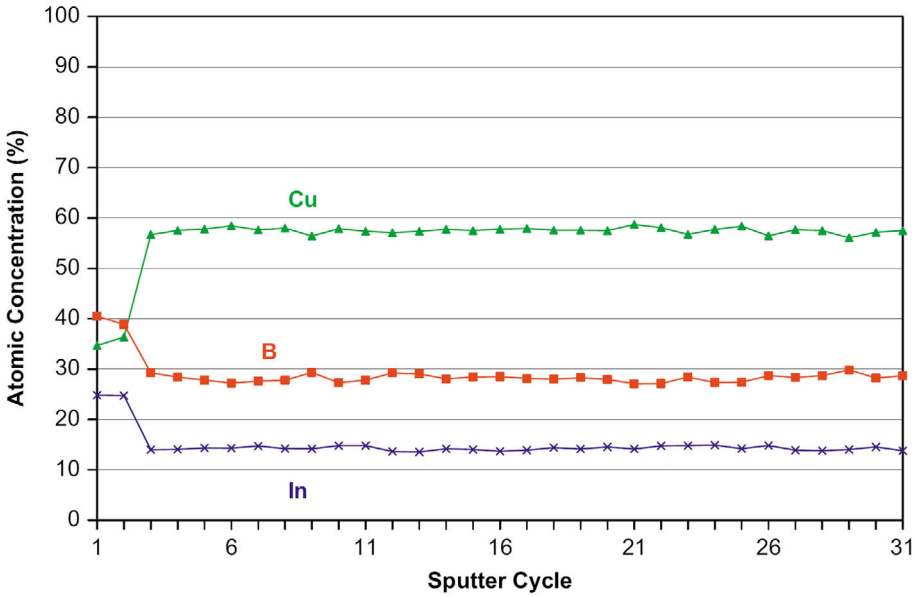

Figure 1. Auger electron spectroscopy depth profile of a co-sputtered Cu, In, B precursor film 070425CIB1 showing uniform distribution of the atomic concentration of each element.

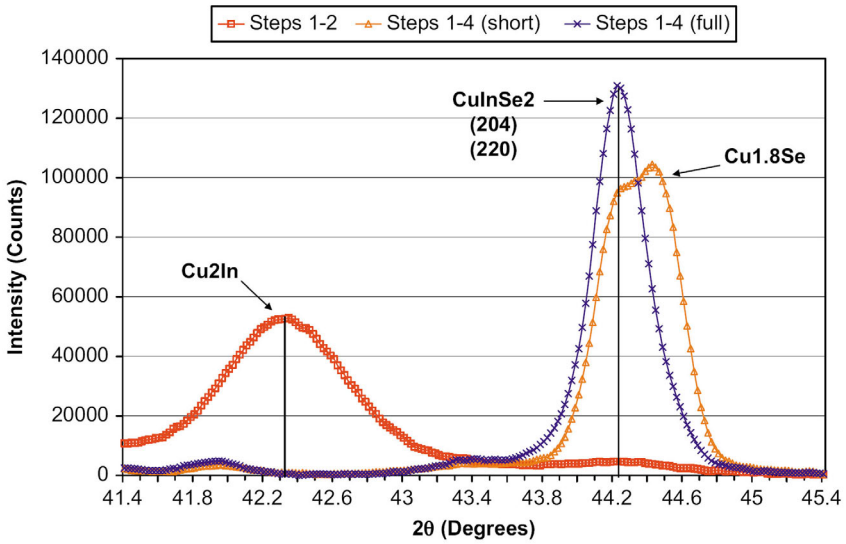

Figure 2. X-ray diffraction of sample 070425CIB1 illustrating the shift in phase as selenization progresses.

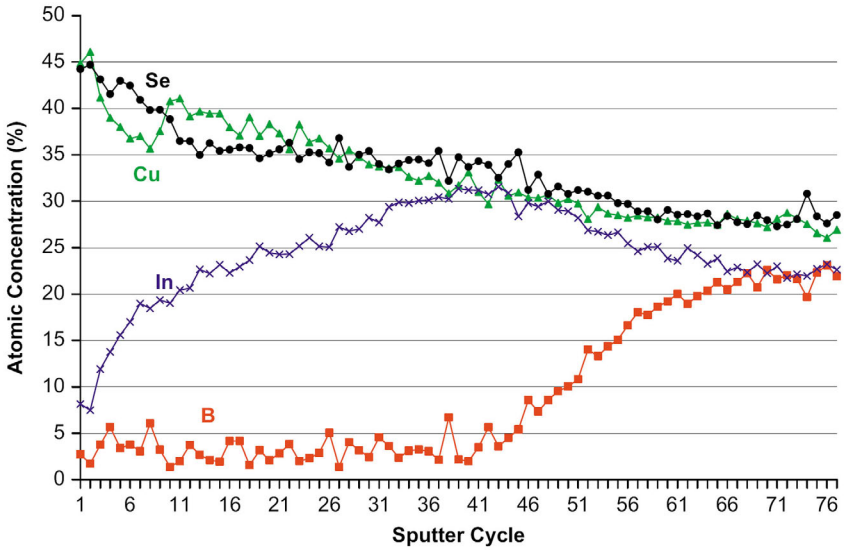

Figure 3. Auger Electron spectroscopy depth profile of a selenized Cu, In, B precursor film 070425CIB1, illustrating the change in atomic concentration from uniformity of the as deposited film to the movement of boron to the film bottom.

substrates were deposited onto simultaneously and were subjected to different durations of the above-mentioned selenization process. XRD measurements were made on these films and the results are displayed in Figure 2. The data depicted by the curve presented as circles is from a sample that only experienced steps 1 and 2 of the selenization process. The curve of triangles is from a sample that experienced steps 1–4 except that step 4 was shortened by 15 min. The final curve, depicted by *x*, is for a sample that fully experienced steps 1–4. Figure 2 suggests that as the selenization procedure progresses, the film slowly changes from a Cu_2In phase, to a $Cu_{1.8}Se$ phase, to the final $CuInSe_2$ phase. Figure 1 shows that the boron was homogenously dispersed in the precursor film.

However, Figure 3 shows that after full selenization, boron can only be found near the back of the film. Note that in all selenized films, the AES sensitivities are uncalibrated, meaning that the depth profile measurements cannot be used to determine exact atomic percentages. AES atomic percentage analysis cannot be easily calibrated because element sensitivities change due to bonding with respect to CIXS composition. However, AES depth profile measurements taken from precursor films are calibrated; therefore these reported atomic percentages are valid.

It was thought that perhaps there was not sufficient boron sputtered into the film in order to properly synthesize CIBS, so a boron rich precursor was made (070718CIB1). The precursor film had a B concentration that was uniformly 55% throughout the film. However, as can be seen in Figure 4 the degree of boron substitution in the precursor does not significantly affect the composition throughout most of the selenized film and the boron again is found only near the back of the selenized film.

To determine if a problem existed in the selenization process, a film of Cu and In was deposited from a $Cu_{0.45}In_{0.55}$ composite target (070228CI1). The resultant selenized film was of uniform composition throughout the film. A look at the XRD results shown in Figure 5 shows that a selenized CuIn film

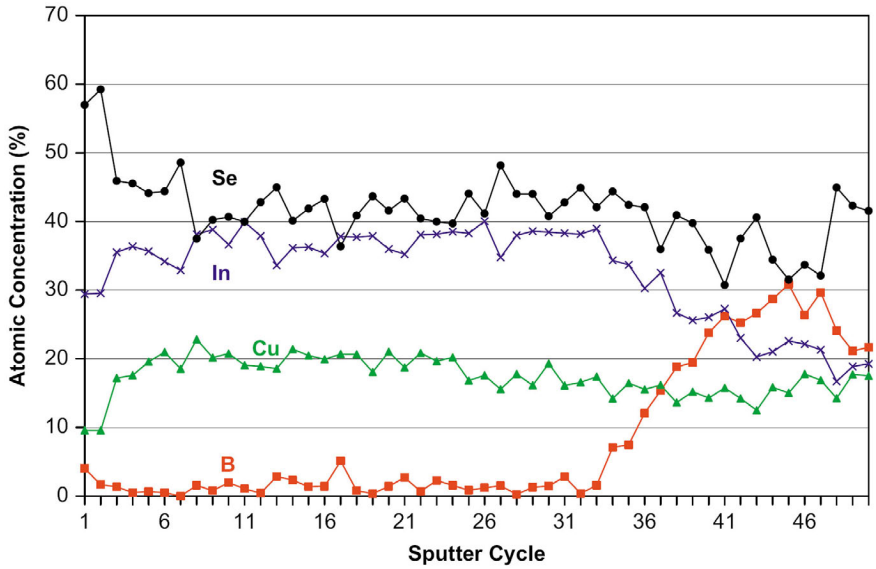

Figure 4. Auger electron spectroscopy depth profile showing the atomic concentration of a boron rich selenized Cu, In, B precursor film 070718CIB1, with boron again accumulating at the bottom of the film.

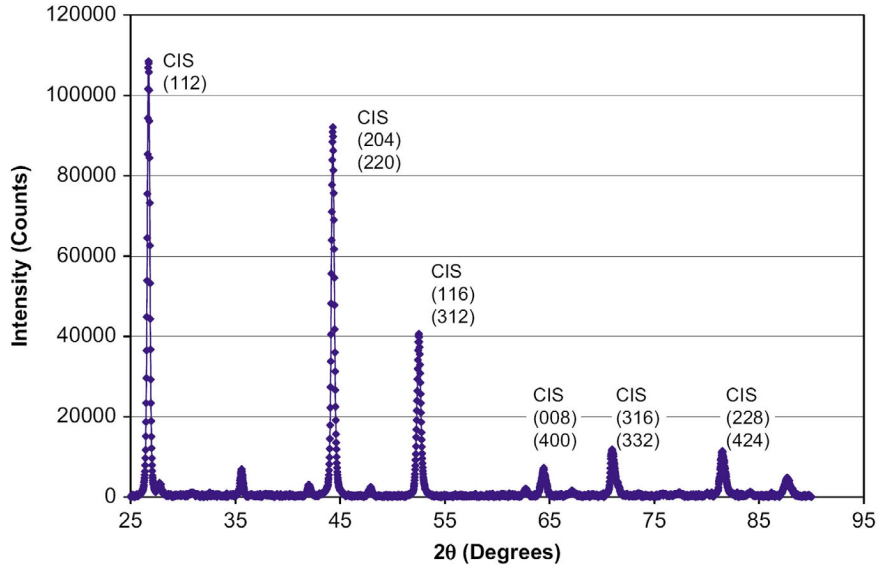

Figure 5. X-ray diffraction results from a Cu–In film selenized using the standard procedure described in the text, the result being a CIS film, sample no. 070228CI1.

does indeed form CIS. The measured 2θ are in exact agreement with the predicted values. Thus, it appears that the standard ex situ selenization procedure that is used is capable of producing quality CIS films and the problem is with the addition of boron in the precursor film.

The next precursor that was deposited consisted of a layer of CuIn sputtered on top of a layer of boron which was sputtered onto the Mo coated substrate (070427CIB1). The AES depth profile of this film was exactly as expected with a mixture of Cu and In on top of B. When this film was selenized what emerged was a layer of Cu, In, and Se on top of a layer of B. It appears that, in this case, the boron serves as a barrier to selenium penetration into the film.

In order to get a better understanding of this phenomenon the next precursor film was deposited with a layer of boron on top of a layer of CuIn on a Mo coated substrate. As expected, the AES analysis showed precursor concentrations exactly as deposited. However, AES of the selenized sample showed that a layer of Cu, In, and Se had formed on top of a layer of B. In all probability, when this particular film was selenized, the CuIn layer diffused through the boron layer, leaving the CuIn-Se_x layer near the surface of the film, and the boron layer at the back of the film was not selenized. This hypothesis is explained below in the description of the selenization process.

As a consequence of the unexpected nature of this result, the deposition profile was repeated. Several samples were examined after different stages in the selenization procedure in order to get a better idea of the progression of the selenization throughout the entire procedure. Figure 6 illustrates the progression of the selenization of the films and the apparent movement of the boron through the films during selenization. Again, these samples were deposited onto simultaneously. Figure 6a shows that after linearly elevating the temperature from room temperature to 250 °C the film is basically unchanged from the precursor, i.e. neither selenization nor atomic movement has occurred. Only a small amount of selenium can

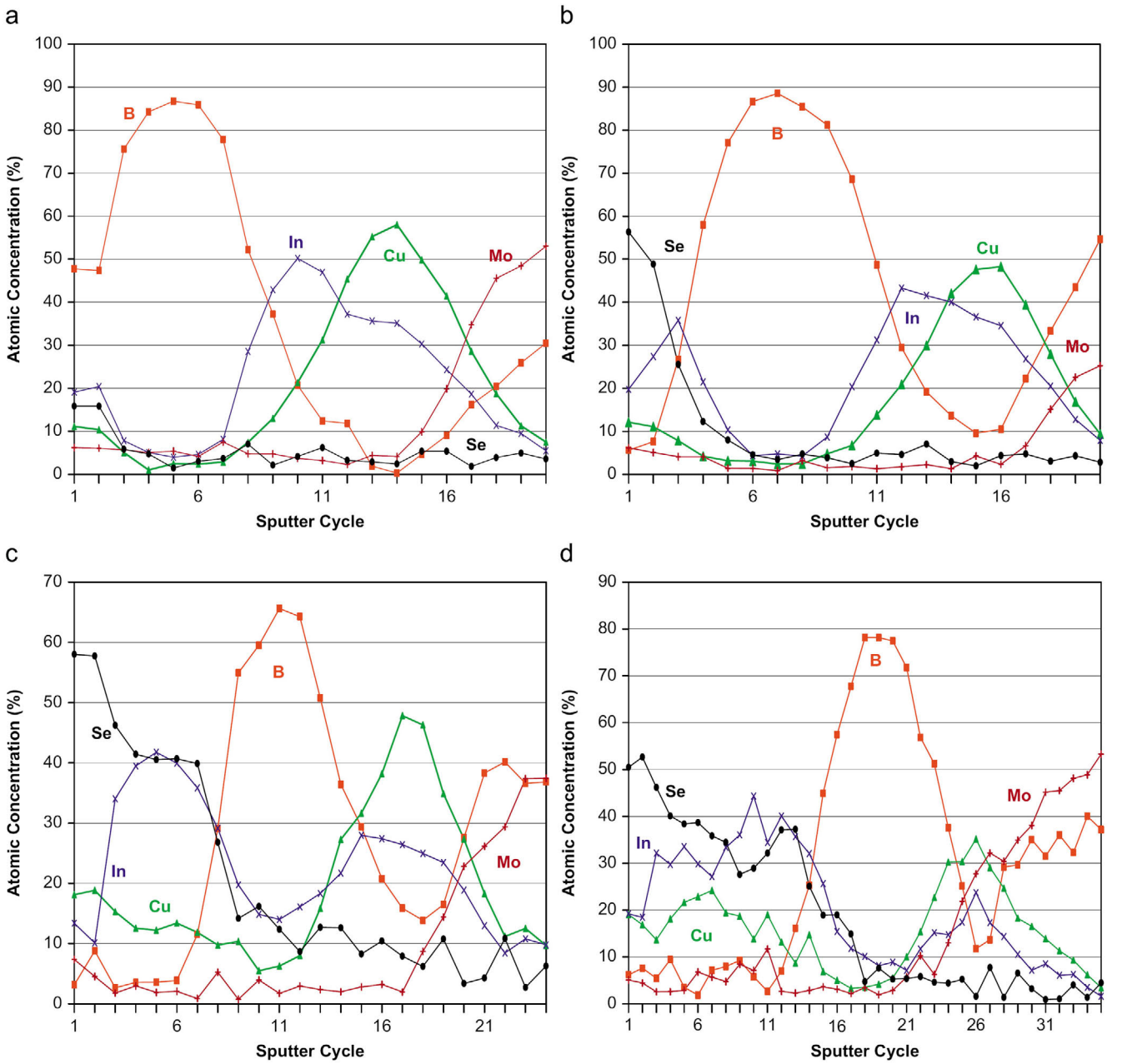

Figure 6. (**a**) Auger electron spectroscopy depth profile of a selenized B on CuIn precursor. The procedure was halted immediately after the temperature was held at 250 °C for 20 min (sample 070810CIB1a). (**b**) AES depth profile of a selenized B on CuIn precursor. The procedure was halted immediately after a temperature ramp to 300 °C after step 2 was completed (sample 070810CIB1b). (**c**) AES depth profile of a selenized B on CuIn precursor. The procedure was halted immediately after a temperature ramp to 350 °C after step 2 was completed (sample 070810CIB1c). (**d**) AES depth profile of a selenized B on CuIn precursor. The procedure was halted immediately after a temperature ramp to 400 °C after step 2 was completed (sample 070810CIB1d).

be found at the surface and none is found in the bulk of the film. However, small amounts of Cu and In have diffused to the film surface. Figure 6b shows what the film looks like after step 2 has been completed and the process is halted after a temperature ramp to 300 °C. The only substantial difference between this stage of the process and the one preceding it is that a significant amount of Se has adhered to the film surface. The AES displayed in Figure 6c has undergone a selenization process identical to that seen in Figure 6b except that the temperature was ramped up to 350 °C before it was allowed to cool. This stage is almost identical to the previous one, except that the boron is now located nearer the bottom of the film at the higher temperature. The AES displayed in Figure 6d is for a sample which has undergone a selenization process identical to that of Figure 6c except that the temperature was ramped up to 400 °C before it was allowed to cool.

The Auger analysis of the film represented in Figure 6d appears to be nearly the same as one which underwent the entire standard selenization procedure. This sequence of selenization runs show that with a B on CuIn layered film, the higher the temperature and the longer the process time, the more Cu and In diffuse to the front of the film, and most of the boron

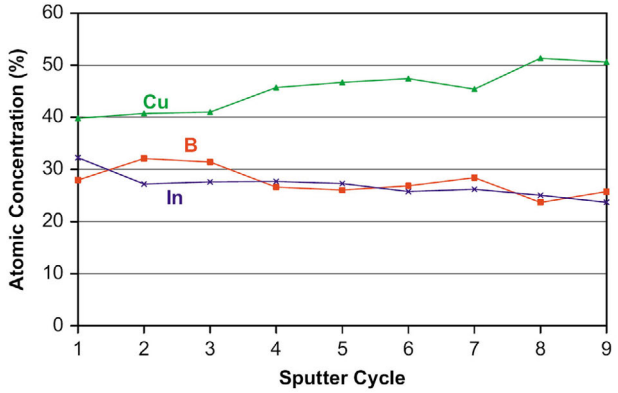

Figure 7. The 6AES depth profile illustrating the atomic concentration of a CIB precursor made from simultaneous deposition of Cu_3B_2 and In targets (070806CIB1).

appears near the back of the film producing a barrier to further Se penetration. The similarity in shape of the boron for each stage of the selenization process indicates that the boron is not the diffusing element, but the Cu and In are diffusing through the boron. Once the melting point of In, T = 156 °C, has been exceeded, numerous Cu–In alloys can be in equilibrium with the molten In and substantial Cu can be dissolved in the In liquid [9] causing the molten alloy to diffuse through the boron.

In another attempt to keep the Cu and B together a CIB precursor was deposited using a Cu_3B_2 target. Although the Handbook of Chemistry and Physics [10] lists a compound Cu_3B_2, the target we purchased, expecting to receive the compound, was a mixture of Cu and B in the above ratio of 3:2. The advantage of this target is that it is able to be DC sputtered, enabling faster deposition times than with the pure B target. A precursor film made from this target along with co-sputtering of In is shown in Figure 7. It can be seen that the ratio of Cu to B is close to the desired value initially and then the ratio of Cu to B becomes smaller. It is obvious that some experimentation with Cu_yB_z must be made before the correct film ratios can be deposited. After selenization, the film had an AES depth profile nearly identical to that of Figure 4, again indicating that the problem is that boron is not being incorporated into the bulk of the film.

4. Conclusions

It appears that it may not be possible to form CIBS films using the precursor deposition and ex situ post-selenization method. All selenized CIBS films, whether co-sputtered from individual targets simultaneously, sputtered in layers, or sputtered from composite targets lack the presence of boron in the bulk of the film. Any boron in these films ends up in a thin region near the substrate interface. Our ability to synthesize quality CIS films using the precursor deposition/ex situ selenization suggest that the procedure is being performed as designed.

In order to more fully investigate whether CIBS films can be formed, other methods must be attempted. The next method would be to deposit the precursor films in an Se vapor as has been done successfully with aluminum [3] as the substitutional atom for indium. It may also be possible to create quality CIBS films using the hollow cathode approach [11]. Electrically excited B and Se ions that would be present in the high energy plasma may have a better chance of reacting to form B and Se bonds. The reason is that there exists a high pressure in the nozzle due to gas flow through it. Homogeneous reaction between B and Se can have high rate in comparison with cases where the pressure decreases, such as in planar magnetron sputtering. [12]

References

[1] M. A. Contreras, K. Ramanathan, J. AbuShama, F. Hasoon, D. L. Young, B. Egass, and R. Noufi, Diode characteristics in state-of-the-art ZnO/CdS/Cu($In_{1-x}Ga_x$)Se_2 solar cells, *Prog. Photovolt Res. Appl.* **13** (2005), p. 209.

[2] S.-H. Wei and A. Zunger, Band offsets and optical bowings of chalcopyrites and Zn-Based II–VI alloys, *J. Appl. Phys.* **78** (1995), p. 3846.

[3] S. Marsillac, P. D. Paulson, M. W. Haimbodi, R. W. Birkmire, and W. N. Shafarman, High efficiency solar cells based on Cu(InAl)Se_2 thin films, *Appl. Phys. Lett.* **81** (2002), p. 1350.

[4] J. T. Heath, J. D. Cohen, and W. N. Shafarman, Defects in copper indium aluminum diselenide films and their impact on photovoltaic device performance, *Mat. Res. Soc. Symp. Proc.* **763** (2002), p. B9.21.

[5] J. H. Yun, R. B. V. Chalapathy, J. C. Lee, J. Song, and K. H. Yoon, Formation of $CuIn_{1-x}Al_xSe_2$ thin films by selenization of metallic precursors in se vapor, *Solid State Phenom.* **124–126** (2007), p. 975.

[6] N. J. Ianno, R. J. Soukup, T. Santero, C. A. Kamler, J. L. Huguenin-Love, S. A. Darveau, J. Olejníček, and C. L. Exstrom, Copper–indium–boron–diselenide absorber materials, *Mat. Res. Soc. Symp. Proc.* **1012** (2007) 1012-T03-21.

[7] A. V. Mudryi, V. F. Gremenok, I.A. Victorov, V. B. Zalesski, F. V. Kurdesov, V. I. Kovalevski, M. Y. Yakushev, and R. W. Martin, Optical characterization of high-quality $CuInSe_2$ thin films synthesised by two-stage selenization process, *Thin Solid Films* **431–432** (2003), p. 193.

[8] R. Caballero and C. Guillén, Optical and electrical properties of $CuIn_{1-x}Ga_xSe_2$ thin films obtained by selenization of sequentially evaporated metallic layers, *Thin Solid Films* **431–432** (2003), p. 200.

[9] N. Orbey, G. A. Jones, R. W. Birkmire, and T. W. F. Russell, Copper indium alloy transformations, *J. Phase Equil.* **21** (2000), p. 509.

[10] C. D. Hodgman, R. C. Weast, and S. M. Selby, *Handbook of Chemistry and Physics* (39th ed), Chemical Rubber Publishing Co. (1957).

[11] R. J. Soukup, N. J. Ianno, and J. L. Huguenin-Love, Analysis of semiconductor thin films deposited using a hollow cathode plasma torch, *Sol. Energy Mater. Sol. Cells* **91** (2007), p. 1383.

[12] Zdenék Hubička, personal communication.